Dual Polarised Reconfigurable Frequency Selective Surfaces

B. Sanz-Izquierdo and E. A. Parker
School of Engineering and Digital Arts, University of Kent, Canterbury CT2 7NT

***Abstract*—Novel band-stop active frequency selective surfaces (FSS) capable of modifying their response for different polarizations are proposed. Geometries based on full rings, and split rings are employed. The designs using full rings are able to tune over a wide frequency range while designs using split rings tune in a narrow frequency band. Both structures use a new biasing methodology which allows independent control of rows and columns of FSS arrays, therefore permitting independent modification of the transmission responses at the vertical and horizontal polarizations. Convoluting the shape of the elements significantly reduces the sensitivity to angle of wave incidence. The aim is to demonstrate a technology that could be used for various applications including modification of the electromagnetic architecture of buildings and the control of electromagnetic wave propagation to improve the efficiency of radio spectrum use. The surfaces incorporate commercially available, low cost, varactor diodes and surface mount resistors. Theoretical and experimental results confirm the operation of the surfaces within the UHF frequency band.**

***Index Terms*— Frequency selective surfaces, PIN diodes, Tuning, Electromagnetic Wave Propagation, EM Architecture**

I. Introduction

The increasing popularity of smartphones and other mobile and wireless devices is stretching data network services to levels never experienced before. Various techniques can improve network capacity including dividing up the spectrum and frequency re-use. In the indoor environment, frequency re-use can be realized by employing frequency selective surfaces, modifying the Electromagnetic Architecture of buildings.

Recent research projects have studied the application of frequency selective surfaces to the built environment [1-2]. Two major challenges for FSS designs for these applications are the long wavelengths at which some of the mobile indoor systems operate [3] - [4] and the high ratio between the frequency bands that may have to be covered [4] - [6]. For example, it might be required to cover the 400MHz European emergency service band and the 2.4GHz Bluetooth band while stopping all intermediate bands, a 6:1 ratio.

Manuscript received March 13, 2013.
The authors are with the School of Engineering and Digital Arts, University of Kent, Canterbury, CT2 7NT, U.K. (e-mail: b.sanz@kent.ac.uk, e.a.parker@kent.ac.uk, j.c.batchelor@kent.ac.uk).

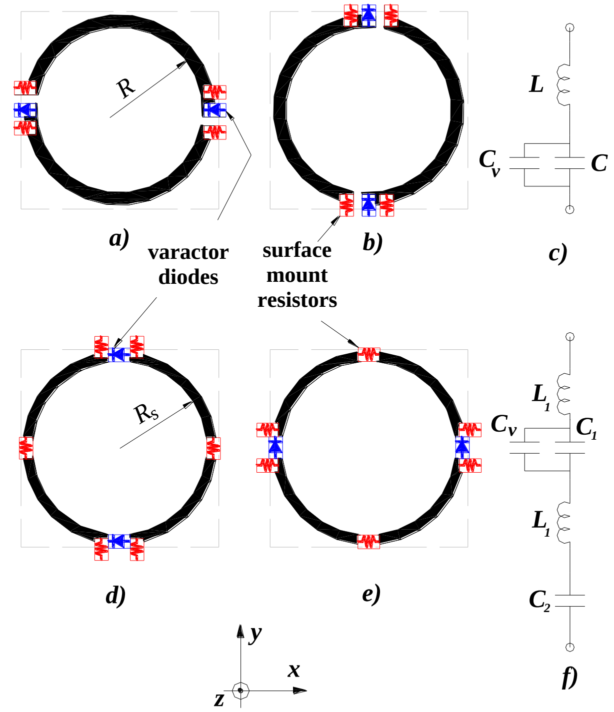

Fig. 1. Active FSS configurations: a) Upper metallization layer for tunable rings. b) lower metallization layer for tunable rings, c) simplified equivalent RF circuit model for tunable rings, d) Upper metallization layer for tunable split rings, e) lower metallization layer for tunable split ring, f) simplified equivalent RF circuit for tunable split rings.

Active frequency selective surfaces (AFSS) enable time varying control over the electromagnetic wave propagation in buildings. Internal areas within the building can be dynamically screened using AFSS, enhancing the capacity for frequency re-use. They can switch between transparent and reflective states at the design frequency, or adjust the phase of the transmission response. Tunable surfaces have the advantage of being able to adapt to future network spectral changes. In addition, they can also compensate for FSS fabrication and installation errors.

Varactor tuned frequency selective surfaces have been reported [7] - [16]. Active band-stop patch [7] – [15] and band-pass slot [16] configurations have been demonstrated. Singly polarized tunable band-stop FSS have been mainly investigated using varactors and transmission lines etched in the same layer [7] - [8]. In [7], a configuration based on split

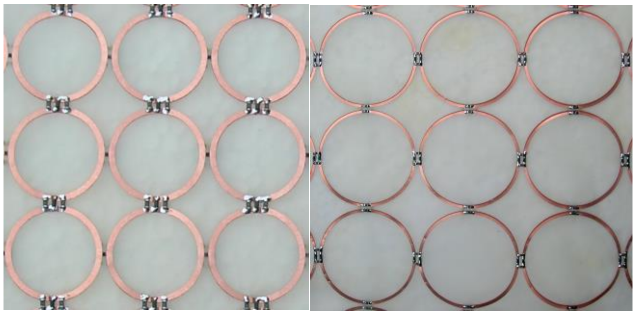

(a) (b)

Fig. 2. Two active FSS configurations: (a) tunable circular loops, (b) tunable split ring

square loops achieved a 6% tuning ratio (normalized difference between the resonant frequencies at maximum and minimum bias voltage), a modest tuning range. This work was extended in [8], where the tuning ratio was improved to about 20% by employing multidiode biasing configurations and adding resistors to compensate transmission distortions arising from the bias circuit. In those papers, the biasing lines extended along the surface, limiting the FSS to singly polarized geometries. Similar configurations were described in [9]-[11], all employing cells with patch pairs and varactors connecting them. There, vias connect the biasing circuit to an external DC control. More recently, a 65% tuning ratio has been achieved [13], though the FSS is singly polarized. A dual polarized tunable band-stop FSS using convoluted dipoles was demonstrated in [14]. The structure consisted of two metallic layers and the biasing circuit is assisted by resistors and metallic vias. There, the tuning ratio achieved was about 8%.

This paper presents novel dual polarized, band-stop tunable FSSs. Two geometries based on rings are analyzed. The first, introduced in section II, is based on circular loops and tunes over a wide frequency range. The second, described in section III, uses split rings and tunes over a narrow frequency range. The two active FSS have in common a novel biasing technology, where diodes and resistors are implemented in two metallic layers sandwiching a very thin, flexible substrate. This creates a double sided structure with high level of re-configuration, which is able to control vertical and horizontal polarizations independently. The behavior of the surfaces over a range of angular illumination and the use of convolution to improve their angular stability are included. The main application is to modify the electromagnetic wave propagation in buildings. Simulation and experiments demonstrate the re-configurable capabilities of the surfaces. The frequency domain solver included in CST Microwave Studio™ was used for the simulations.

II. Tunable Circular Loop

A. Design and analysis

The circular loop or ring is a well known FSS element geometry, constituents of arrays characterized by having good angular stability and dual polarization performance [17]. The structure typically resonates at a circumference of λ, the incident wavelength, making a relatively compact element. When excited by a linearly polarized plane wave, the current density of the rings has nulls in the sections perpendicular to the incident electric field [18].

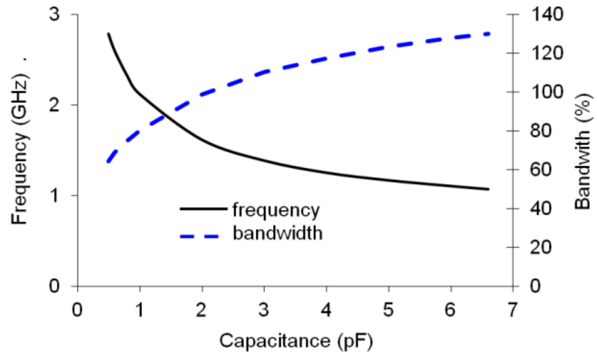

Fig. 3. Simulated resonant frequency and -10dB bandwidth at normal incidence of the tunable ring for various values of varactor capacitance

A novel active FSS using ring elements has been created by etching split ring patterns on the two metallic layers of a double layer structure sandwiching a 0.05mm thick polyester substrate (Mylar). The split ring patterns are identical but rotated by 90 degrees from each other. Fig.1 a) and b) illustrate the front and the rear of the FSS. Fig.2 a) shows a photograph of a 3x3 element array. The FSS itself consisted of a 10 x 10 array on a rectangular lattice of periodicity P = 19mm. Diodes and resistors were added at the end of the split rings, connecting adjacent elements. The diodes chosen were the BB857 silicon varactors with a tunable capacitance range from 0.5pF (28V) to 6.6pF (1V), and the resistors were of 10kΩ. In DC, the circuit consisted of transmission lines with resistor pairs connecting varactor diodes in parallel configuration. As in [13], [14], the resistors produce a voltage drop, which in our case was of about 0.1% per cell. This value is not very significant for the actual array size but could limit the performance if applied to large arrays. Alternative options such as chip inductors [19] offer low resistance at DC and high impedance at RF but they are constrained by their narrow frequency operation.

When excited by an RF plane wave, each element behaves as a single layer ring structure owing to the very low impedance between the capacitively coupled ring surfaces on the two sides of the dielectric substrate. The capacitance between ring quadrants can be determined from the equation:

$$C_{coupling} = \varepsilon_r \varepsilon_0 \frac{A}{d} \approx \varepsilon_r \varepsilon_0 \frac{\pi\left(R_e^{\,2} - R^2\right)}{4d} \qquad (1)$$

where R_e is the outer radius of the ring, R the inner radius, and d is the thickness of the dielectric substrate. The dimensions of the design presented here are: R_e = 9.1mm, R = 8 mm, d = 0.05mm, ε_r = 3. This gives a capacitance of $C_{coupling}$ = 7.8 nF and an impedance at 1GHz of 0.02 ohms.

An equivalent circuit model of square loop elements was described in [20]. A similar model (Fig.1c)) can be applied to the circular loop design here when is vertically polarized and the capacitance of the diodes ($C_{v)}$ in the layer in Fig.1b) are varied, or when horizontally polarized and the diodes in the layer in Fig.1a) are modified. L is the inductance due to the circular loop and C is the capacitance between adjacent elements. The resonant frequency of this structure is given by the equation:

$$f_o = \frac{1}{2\pi\sqrt{L(C_v + C)}} \approx \frac{1}{2\pi\sqrt{LC_v}} \quad (2)$$

Computational results of the effect of varying the capacitance of the varactor diodes on the resonant frequency and bandwidth are shown in Fig.3. Diodes were added as lump capacitors in these calculations. When they were not included, the FSS resonated for a ring circumference of about λ [17] with 1.5% and 3% shift in resonant frequency at TE45 and TM45 respectively. When the rings were loaded with the capacitance of the varactor diode at 28V (0.5pF), the FSS resonated at a ring circumference of about $\lambda/2$ and unit cell size of $(0.176\lambda)^2$, with a frequency drift of less than 3% at TE45 and 10% at TM45. When loaded with the capacitance of the diode at 1V (6.6pF), the FSS resonated at a ring circumference of about $\lambda/5$ and unit cell size of $(0.068\ \lambda)^2$, with the resonant frequency shifting by less than 2% at TE45 and 10% at TM45. The total change in resonant frequency corresponds to a tuning ratio $((f_{max}-f_{min})/f_{centre})$ of over 80%, which confirms that the FSS is very sensitive to changes in C_v, as expected from equation (2).

It should be noted here that the capacitance resulting from changes in the reverse voltage applied to the varactor diodes [21] is characterized by a rapid decreased for voltages from 1V (6.6pF) to about 9V (≈1pF) and a slow decrease from 9V (≈1pF) to 28V (0.5pF). This compensates the curve of the active FSS for different capacitance values (Fig.3) and creates a more linear change of the resonant frequency with bias voltage as described in the following section.

B. Measurements

Measurements were carried out using two log periodic antennas at 0.6 m from the center of the FSS. The FSS was placed in an open aperture of approximately 190 x 190 mm, surrounded by an absorbing wall of 3m by 3m. Swept frequency transmission responses were calibrated against the open aperture. This arrangement was able to predict well the full plane wave behavior of active FSS in previous work [4], [22]-[23].

Figs.4, 5 and 6 show the measured transmission responses at normal incidence, TE45 and TM45 when the voltage of the diodes was varied from 1 V to 28V. For clarification, in the vertical polarization (Fig.1) the E-field remains in the yz plane, so for example in TM the direction of wave incidence is also in yz. The approximate equivalent capacitance for the various voltage values as extracted from the datasheet were as follows: 28V=0.5pF, 20V=0.63pF, 15V=0.75pF, 10V=0.95pF, 5V=2.3pF and 1V=6.6pF. A wide band tuning ratio of over 65% was observed, with the shape of the band-stop filter degrading gradually as the voltage across the varactor decreased. Internal losses of the diodes and the lower quality factor of the LC circuit clearly affected performance for large values of varactor capacitance. The resistors of the biasing circuit and the dielectric material employed also add losses to the structure. In addition, there was a frequency shift relative to normal incidence illumination of about 5% at TE45 and 10% at TM45. Simulation and measurement results show that the incorporation of the varactors or any capacitive component in the annular loop array degrades the angular stability at TM incidence, owing to changes in the component of the E-field between the regions in the diodes that lead to their effective capacitance. A solution to the fairly poor angular stability of capacitive loaded loops is described in the following subsection.

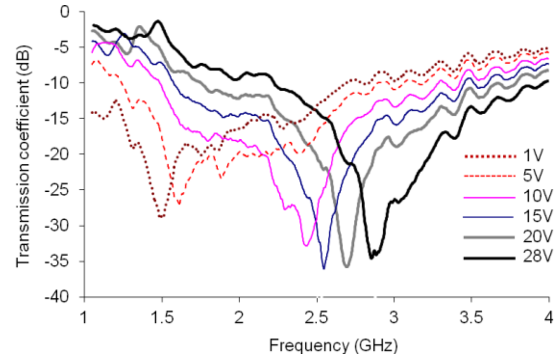

Fig. 4. Measured transmission responses of the tunable ring at normal incidence

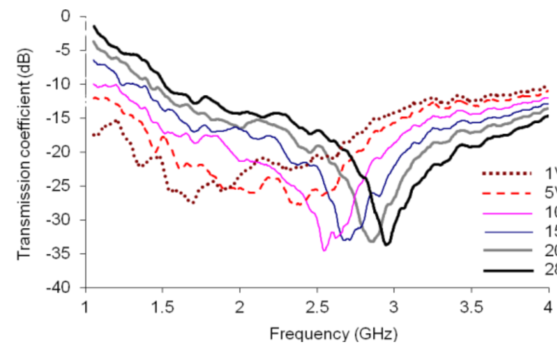

Fig. 5. Measured transmission responses of the tunable ring at TE45

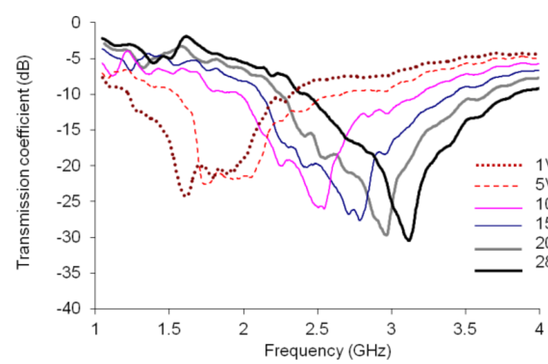

Fig. 6. Measured transmission responses of the tunable ring at TM45

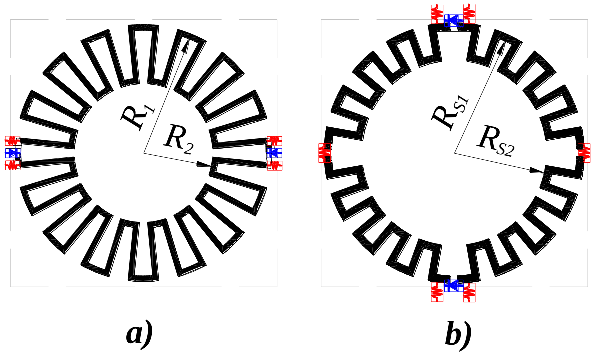

Fig. 7. Upper metallization layers for tunable FSSs. a) convoluted ring, b) convoluted split rings

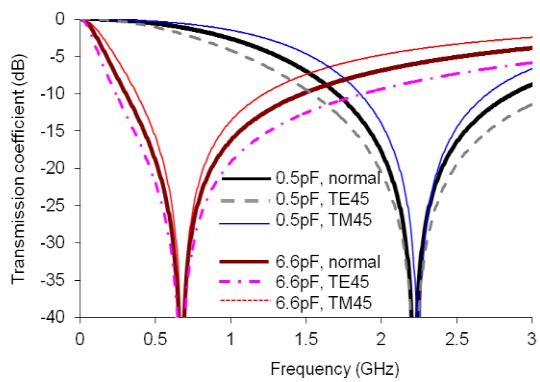

Fig. 8. Simulated transmission responses at normal incidence of convoluted ring for varactor diode capacitance of 0.5pF and 6.6pF

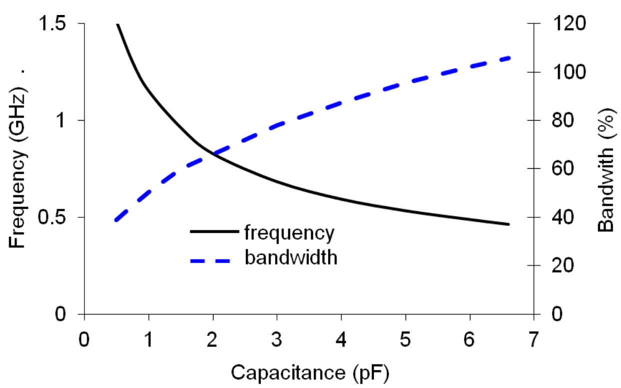

Fig. 9. Resonant frequency of the convoluted ring at normal incidence when the number of stubs is increased from 0 to 16.

C. Convoluted active circular loop

Convoluting the elements of an FSS is a technique able to reduce the size of the unit cell and improve the angular stability of the frequency responses [4], [24] - [26]. This technique has been applied to the tunable circular loop in Fig.1 a) with the aim to reduce the frequency shift at different angles of illumination. The resulting structure after convolution is shown Fig. 7 a). Stubs were added every 22.5^o of the circular loop, making a total of 16 stubs. As with the original circular loop element (Figs.1 a) and b)), the top split ring overlaps the lower level split ring to create a full ring at RF. The main dimension of the novel convoluted structure were: R_1 = 9 mm, R_2 = 5 mm and width of the conductor w = 0.38mm. The periodicity of the unit cell was kept at P = 19mm.

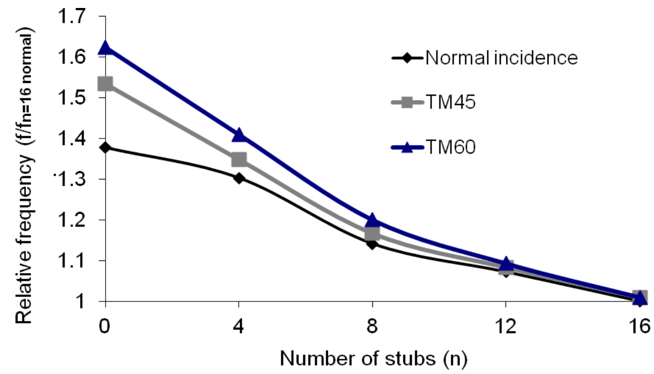

Fig. 10. Computed effect on frequency at normal incidence, TM45 and TM60 of adding stubs to the active ring FSS

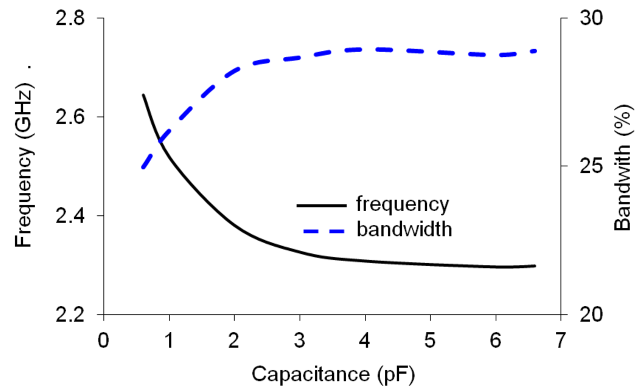

Fig. 11. Computed dependence of resonant frequency and -10dB bandwidth of the tuneable split ring on varactor diode capacitance, normal incidence

The unloaded convoluted ring resonated for a unit cell size of $(0.186\,\lambda)^2$ with a frequency shift of 0.3% at TE45 and 0.5% at TM45. When the ring was loaded with capacitive values of 0.5 pF and 6.6pF, the FSS resonated for unit cell dimensions of $(0.096\lambda)^2$ and $(0.03\lambda)^2$ respectively (Fig.8 and 9). The shift in resonant frequency at TE45 and TM45 was below 1% for the convoluted ring loaded with lump elements of capacitance between 0.5pf to 6.6pF. A tuning ratio of over 100% was achieved in the simulation, which is almost 20% higher than that of the unconvoluted design. The -10dB bandwidth of the convoluted structure was 25% lower than that for the unconvoluted one.

A further parametric analysis was carried out on the effect of convoluting on angle of incidence performance. Circular loops end loaded with 0.5pf capacitors were used for the comparison. Fig.10 shows the effect of adding stubs to the resonant frequency at normal incidence, TM45 and TM60. The shift in resonant frequency at TM60 decreased from 17% for no stubs to less than 0.5% for n = 16 stubs, with the highest improvement observed between 0 and 4 stubs. In the TE case in these calculations, the frequency drift at TE45 and TE60 was less than 1%. Note that the y-axis has been normalized to the resonant frequency at normal incidence for n = 16 stubs.

III. DUAL POLARISED TUNABLE SPLIT RING

A. *Design and analysis*

The effect on the transmission responses of breaking the conductor of loop elements was studied in [18], [27]. The resulting resonant frequency depends on where the loop is cut with respect to its sinusoidal current distribution. For the FSS design here, a circular loop has been split into four equal segments as illustrated in Fig. 1 d) and e). The resulting element is dual polarised and resonates at a frequency which is about twice that of the full ring. Independent tuning for vertical and horizontal polarisation can be achieved by using two identical layers sandwiching a very thin substrate, with varactor diodes and resistors pairs in the lower metallization layer (Fig.1 e)) rotated 90 degrees with respect to the upper layer (Fig.1. d)). This configuration creates a DC circuit consisting of varactors connected in parallel through transmission lines with resistor pairs. The circuit in the layer in Fig.1e) controls operation at vertical polarization (E-field in yz) while the circuit in Fig. 1d) controls horizontal polarization operation (E-field in xz).

A simplified equivalent circuit model of the active FSS at RF is shown in Fig.1 f)), also described for a single polarised active configuration in [28]. In contrast to the design in section II, the varactor is in series with C_2 in the equivalent circuit, reducing the effect of the capacitance of the diode C_v in the resonant frequency. The resonant frequency is given by:

$$f_0 \approx \frac{1}{2\pi\sqrt{(2L_1)\left(\frac{(C_V+C_1)\cdot C_2}{C_V+C_1+C_2}\right)}} \qquad (3)$$

where L_1 is the inductance due to vertical segments of the split ring, C_1 is the capacitance between the two vertical elements and C_2 the capacitance with elements of adjacent unit cells. Note that the internal resistance of the capacitor has not been included in the model owing to its low impedance value in relation to the impedance of C_v and C_2 [28].

In order to verify the behaviour of the FSS, the tunable design was simulated using the frequency domain solver included in CST Microwave studio™. The main dimensions were: radius of the inner circle R_s = 17.25 mm, width of the patch w = 1mm, width of split s = 1mm, periodicity P = 37.5mm, substrate thickness t_h =0.05mm, substrate permittivity ε_r=3.0.

Fig. 11 shows the effect of varying the diode capacitance between 0.5pF and 6.6pF on the resonant frequency. The unloaded split ring resonated for a unit cell size of $(0.6\ \lambda)^2$, with a frequency drift of about 7.5% at TE45 and TM45. When loaded with 0.5pF, the FSS resonated for a unit cell size $(0.37\lambda)^2$ with a frequency drift of 2.4% at TE45 and 6.4% at TM45. When loaded with the maximum capacitance of the varactor diodes (6.6pF) the FSS resonated for unit cell size of $(0.27\lambda)^2$ with a frequency drift of 2.4% and 5.4% at TE45 and TM45 respectively. The tuning ratio achieved was about 16%, confirming that the effect of C_v is significantly reduced by the series capacitance C_2, as expected from equation (3).

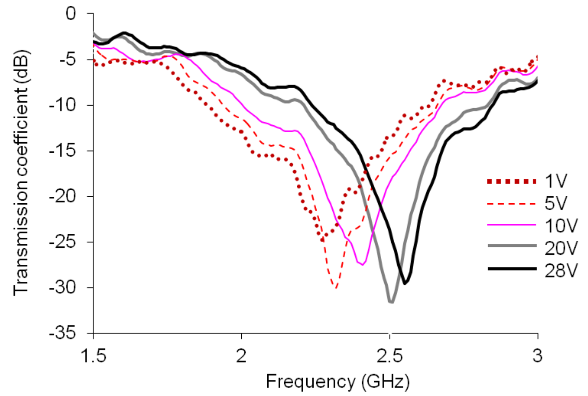

Fig. 12. Measured transmission responses at normal incidence of the tunable split ring FSS

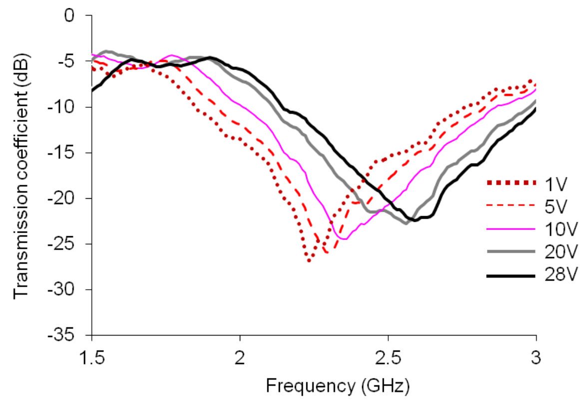

Fig. 13. Measured transmission responses of the tunable split ring at TE45

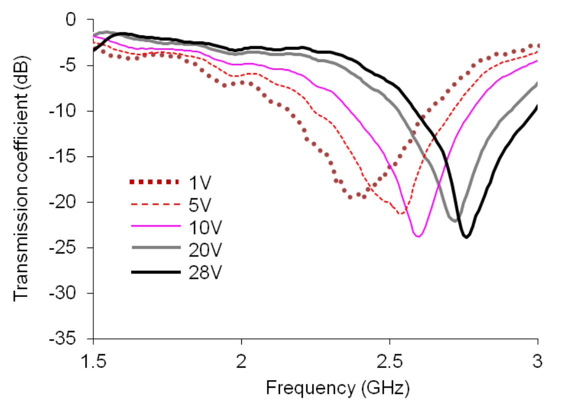

Fig. 14. Measured transmission responses of the tunable split ring at TM45

B. *Measurements*

A 5x5 array of active split rings was etched on each side of a double sided polyester substrate. Diodes and resistors were inserted and soldered to the surface as shown in Fig. 2 b). The final structure was then measured in a plane wave chamber.

Figs.12, 13 and 14 show the measured transmission responses at normal incidence, TE45 and TM45 respectively. Tuning over a frequency range of about 15% was observed. When 28V (≈0.5pF) were applied to the varactor diodes, the FSS resonated at about 2.6GHz with a frequency drift of about

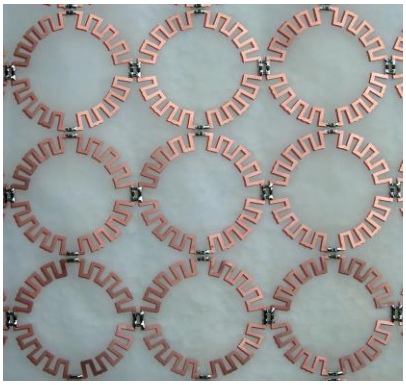

Fig. 15. Tunable convoluted split rings

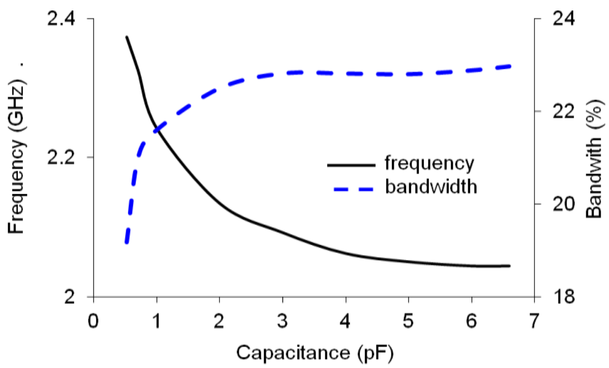

Fig. 16. Computed resonant frequency and -10dB bandwidth of the tunable convoluted split ring as functions of varactor diode capacitance, normal incidence

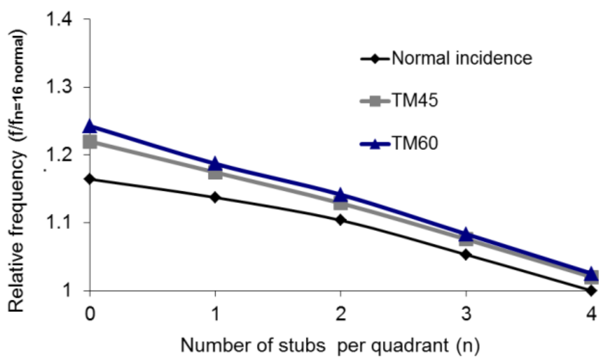

Fig. 17. Computed effect of adding stubs to the active split ring FSS on resonant frequency at normal incidence, TM45 and TM60

2.5% at TE45 and 8% at TM45. When 1 V (≈6.6pF) was applied resonance occurred at 2.25GHz with a frequency drift of less than 1% at TE45 and 6% at TM 45. The main differences between the simulation and measurements relate to the physical characteristic of the diodes and resistors and the losses of the components and dielectric material. As the drift in angle of incidence was significant, it was decided to apply convoluting techniques to the active split ring array structure. This is described in the following subsection.

C. Convoluted active split rings

Similarly to the structure described in section II.C, convolution was applied to the split rings by adding stubs perpendicular to the loop. Every quadrant of the split ring was convoluted as shown in Fig. 7 b). Four stubs were added per segment, which were placed at 22.5º from each other. The main dimensions of the convoluted element were: outer radius R_{S1} = 17.25mm, inner radius R_{S2} = 13mm, strip line thickness t_h = 1mm and periodicity P = 37.5mm.The unloaded convoluted split ring structure resonated at a unit cell size of $(0.46\ \lambda)^2$ with frequency shift of 2.7% at TE45 and 3.6% at TM45.

The effect of varying the capacitance of the varactor diodes on frequency and bandwidth was simulated and the results are shown in Fig 16. When the split ring was loaded with a capacitance of 0.5pF, the FSS resonated for a unit cell size of about $(0.3\lambda)^2$ with 2% frequency drift at TM45 and less than 0.5% at TE45. When a load of 6.6pF was applied to the structure, the FSS resonated for a unit cell size of $(0.26\lambda)^2$, with a frequency shift of 1.8% at TM45 and 0.5% at TE45. The total tuning ratio achieved with this structure was 16%, which is about the same ratio as that of the unconvoluted structure.

A study of the effect of adding stubs to the element on resonant frequency and stability to angle of illumination was carried out and the results are illustrated in Fig.17. One to four stubs in step of 1 stub were added to the split ring structure loaded with lump elements of 0.5pF. As expected, adding stubs significantly improved the angular stability at TM45 and TM60 but 4 stubs were still insufficient to reduce the drift at TM60 below 1%. The performance at TE60 was significantly better with frequency drift decreasing from about 5% for no stubs to less than 0.5% for 4 stubs.

D. Convoluted active split rings -measurements

A 5x5 array of the convoluted split rings was etched on each metal clad layer of a double sided polyester substrate. Fig.15 shows 3x3 elements of the top layer of the structure. Figs. 18, 19 and 20 show the measured transmission responses at normal incidence, TE45 and TM45. It can be observed that the structure is significantly more stable to angle of incidence than the unconvoluted split ring strucure reported in section III.B. When 28V (≈0.5pF) were applied to the varactor diodes, the FSS resonated at about 2.35GHz with frequency drifts below 1% at TE45 and TM45. When 1 V (≈6.6pF) was applied, resonance occurred at about 2 GHz with a frequency drift a less than 2% at TE45 and TM 45. The resonant frequencies were between 1% and 3% lower than those obtained in the simulation (Fig.16).

E. Independent polarization control

Virtually independent tuning in the vertical and horizontal polarizations was observed with all the FSS arrays described in this paper. As a demonstration, a set of four measurements at TM45 with different voltages for vertical and horizontal polarizations is shown in Fig.21. The measurements relate as follows: 28V_28V is the case where 28V was applied to all diodes simultaneously, 28V_01V relates to 28V applied to the (y-directed) diodes in Fig.1e) and 1V to those in in Fig.1d), and so on. With a constant voltage applied to the y-directed diodes, only a very small change in the resonant frequencies and shape of the transmission curves was observed for changes in voltages in the x-directed ones.

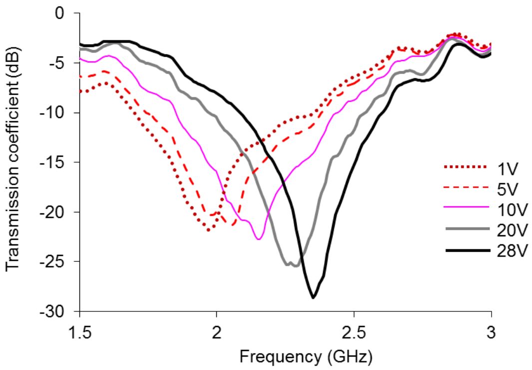

Fig. 18. Measured transmission responses at normal incidence of the convoluted split ring

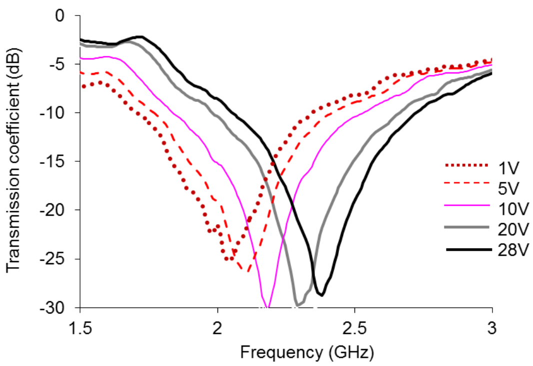

Fig. 19. Measured transmission responses at TE45 of the convoluted split ring

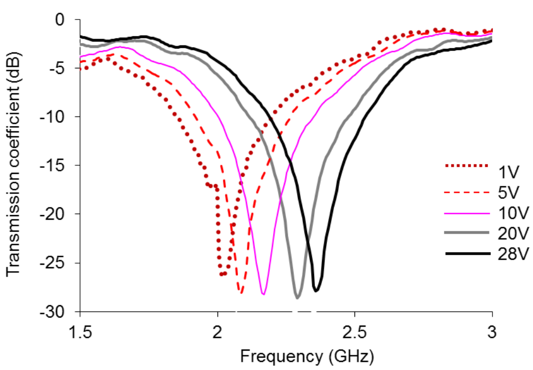

Fig. 20. Measured transmission responses at TM45 of the convoluted split ring

IV. Conclusions and Discussion

Novel dual polarized tunable frequency selective surfaces based on band stop elements have been presented. The structures employ two metallic layers sandwiching a very thin substrate to achieve independent tuning for vertical and horizontal polarizations. This could have advantages in systems where peak transmission levels differ in the vertical and horizontal polarizations, thus improving the filtering characteristics of the FSS. The configurations presented here are based on full rings and split rings. Full rings were able to tune over a wide frequency range while split rings for a small range of frequencies. The incorporation of active capacitive

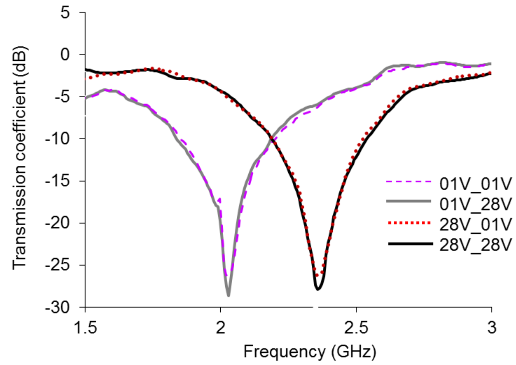

Fig. 21. Effect of changing bias voltages across the x-directed diodes for constant voltages across the y-directed diodes, TM45

elements such as varactor diodes degrades the angular stability of the FSS structures. Convoluting the active structures has been demonstrated to be a good solution to the drift at different angles of illumination. As with typical FSS elements, convolution decreased the resonant frequency and -10dB bandwidth. A tuning range ($(f_{max}-f_{min})/f_{centre}$) of over 65% can be achieved using circular loops and over 15% using split rings. CST Microwave Studio™ simulations where diodes were added as lump elements predicted well the tuning characteristics, but inclusion of the full physical dimensions of the components may be necessary to obtain a more accurate prediction of losses in the structure (Section II.B). Higher quality diodes could also be employed to improve performance. The roll-off rate and therefore the filtering characteristics of the active FSS could be further improved by cascading layers of active FSS. These active frequency surfaces are intended for controlling the electromagnetic architecture of buildings where relatively small interference attenuation can result in significant improvement in system outage probability [29].

V. Acknowledgment

The authors would like to thank Dr. John Batchelor for useful discussions. They also thank Simon Jakes for assisting in the fabrication of the FSS.

References

[1] M. Philippakis, C. Martel, D. Kemp, R. Allan, M. Clift, S. Massey, S. Appleton, W. Damerell, C. Burton, and E.A. Parker, "Application of FSS structures to selectively control the propagation of signals into and out of buildings", Ofcom ref. AY4464A, 2004 [Online]. Available: http://stakeholders.ofcom.org.uk/binaries/research/spectrum-research/exec_summary.pdf

[2] M. Hook and K. Ward, "A project to demonstrate the ability of frequency selective surfaces and structures to enhance the spectral efficiency of radio systems when used within buildings", Ofcom ref. AY4462A, 2004.

[3] E.A. Parker, J.B. Robertson, B. Sanz-Izquierdo and J.C. Batchelor, "Minimal Size FSS for Long Wavelength Operation". *Electron. Lett.*, vol.44, no.6, pp. 394-395, March 2008

[4] B. Sanz-Izquierdo, E.A. Parker, J.-B. Robertson, J.C. Batchelor, "Singly and Dual Polarized Convoluted Frequency Selective Structures", *IEEE Trans. Antennas and Propagat.*, vol. 58, no. 3, pp. 690-696, March 2010

[5] B. Sanz-Izquierdo, I.T. Ekpo, J.-B. Robertson, E.A. Parker and J.C. Batchelor, "Wideband EM Architecture of Buildings: Six-to-One Dual-Passband Filter for Indoor Wireless Environments", *Electron. Lett.*, vol.44, no.21, pp. 1268-1269, 2008

[6] B. Sanz-Izquierdo, J.B. Robertson, E.A. Parker and J.C. Batchelor, "Double Layer Interwoven Frequency Selective Surfaces", *Proc. 3rd European Conference on Antennas and Propagation, EuCAP* 2009, Berlin, pp. 1914-1917

[7] C. Mias, "Waveguide and free-space demonstration of tunable frequency selective surface" *Electron. Lett*., vol. 39, no.14, pp.1060–1062, July 2003

[8] C. Mias, "Demonstration of Wideband Tuning of Frequency-Selective Surfaces in a Waveguide Set Up" *Microwave and Optical Technology Letters*, vol. 44, no.5, pp. 412 – 416, Wiley, March 2005

[9] S.V.Humm, M. Okoniewski and R.J. Davies, 'Realizing an electronically tunable reflectarray using varactor diode-tuned elements', *IEEE Microw. Wirel. Compon. Lett.*, vol.15, no.6, pp. 422–424, 2005

[10] S.V.Hum, , M.Okoniewski and R.J.Davies,: 'Modeling and design of electronically tunable reflectarrays', *IEEE Trans. Antennas Propag*., vol. 55, no.8, pp. 2200–2210, 2007

[11] A.R.Weily, , T.S. Bird, , and Y.J. Guo,: 'A reconfigurable high-gain partially reflecting surface antenna', *IEEE Trans. Antennas Propag*., vol. 56, no.11, pp. 3382–3390, 2008

[12] A. Tennant and B. Chambers, "A single-layer tuneable microwave absorber using an active FSS", *IEEE Microwave and Wireless Components Letters*, vol. 14, no. 1, p.p. 46 – 47, Jan. 2004

[13] B. Sanz-Izquierdo, E.A. Parker, J.B.Robertson and J.C.Batchelor, "Tuning patch-form FSS" *Electron. Lett*., Vol. 46, no. 5, p.329–330. 4 March 2009

[14] C. Mias, "Varactor-Tunable Frequency Selective Surface with Resistive-Lumped-Element Biasing Grids", *IEEE Microw. and Wireless Component Lett*. vol. 15, no.9, 570-572, Sept. 2005.

[15] C. Mias and C. Tsakonas, "Waveguide Demonstration of Varactor-Diode-Tunable Band-Pass Frequency Selective Surfaces", *Microwave and Optical Technology Letters*, vol. 45, no.1, pp. 62 – 66, Wiley, 25 Feb 2005

[16] B. Sanz-Izquierdo, E.A. Parker, J-B. Robertson and J.C. Batchelor, "Tuning Technique for active FSS Arrays", *Electron. Lett*., vol. 45, (22), p.1107–1109. 22 October 2009

[17] E.A. Parker and S.M.A. Hamdy, "Rings as Elements for Frequency Selective Surfaces", *Electron. Lett*., vol. 17, pp. 612-614, 1981

[18] A.D. Chuprin, E.A. Parker and J.C. Batchelor, "Resonant Frequencies of Open and Closed Loop FSS Arrays," *Electron. Lett.*, vol. 36, no.19, pp 1601-1603, Sept. 2000

[19] P.S. Taylor, E.A. Parker and J.C. Batchelor " An Active Annular Ring Frequency Selective Surface", *IEEE Trans. Antennas Propag*., vol. 59, no.9, pp. 3265 – 3271, 2011

[20] R.J. Langley and E.A. Parker, "Equivalent Circuit Model for Arrays of Square Loops" *Electron. Lett.*, vol. 18, pp 294-296, 1982

[21] [online]Available:http://www.infineon.com/dgdl/bb837_bb857series.pdf?folderId=db3a304313d846880113d94414f400fc&fileId=db3a304313d846880113d97339a9011a (Accessed Feb. 2013)

[22] B. Sanz-Izquierdo, E.A. Parker and J.C. Batchelor, 'Switchable Frequency Selective Slot Arrays', *IEEE Transactions on Antennas and Propagation*, vol.59, no.7, pp. 2728 – 2731, 2011

[23] B. Sanz-Izquierdo, E. A. Parker, and J. C. Batchelor, "Dual-band tunable screen using complementary split ring resonators," *IEEE Trans. Antennas Propag*., vol. 58, no.11, pp. 3761–3765, Nov. 2010.

[24] E. A. Parker and A. N. A. El Sheikh, "Convoluted array elements and reduced size unit cells for frequency-selective surfaces," *IEE Proc. H: Microwaves, Antennas, and Propagation*, vol. 138, pp. 19–22, Feb. 1991.

[25] E.A. Parker, A.N.A. El Sheikh and A.C. Lima, "Convoluted frequency-selective array elements derived from linear and crossed dipoles", *IEE Proc. H*, vol. 40, no.5, pp. 378–380, 1993

[26] E.A. Parker and A.N.A. El Sheikh, "Convoluted dipole array elements", *IEE Electron. Lett*., vol. 27, no.4, pp. 322–323, 1991

[27] A.E Martynuk A.E, and J.I. Martinez Lopez, "Frequency selective surfaces based on shorted ring slots," *Electron. Lett*., vol. 37, pp.268-269, 2001

[28] T.K. Chang, R.J. Langley and E.A. Parker, "An active square loop frequency selective surface", *IEEE Microwave and Guided Wave Letters*, vol. 3, no. 10, pp.387 - 388, Oct. 1993

[29] A. H.Wong, M. J. Neve, and K. W. Sowerby, "Performance analysis for indoor wireless systems employing directional antennas in the presence of external interference," in Proc. IEEE AP-S Int. Symp., Washington, DC, vol. 1A, pp. 799–802, 2005

Benito Sanz Izquierdo received the B.Sc. from the University of Las Palmas de Gran Canaria, and the M.Sc. and Ph.D. degrees from the University of Kent, Kent, U.K., in 2002 and 2007 respectively.

From 2003 to 2012, he was a Research Associate with the School of Engineering and Digital Arts, University of Kent, and in 2013, became a lecture in Electronic Systems. In 2012, he spent some time working for Harada Industries Ltd where he developed novel antennas for the automotive industry. His research interests are multiband antennas, wearable microwave devices, substrate integrated waveguides components, electromagnetic band-gap structures and frequency selective surfaces.

Edward (Ted) Parker graduated from St Catharine's College, Cambridge University, U.K., with an MA degree in physics and PhD in radio astronomy. He established the antennas group in the Electronics Laboratory at the University of Kent, U.K. The early work of that group focused on reflector antenna design, later on frequency selective surfaces and patch antennas. Ted is a member of the IET. One of his interests is the study and overhaul of antique clocks. He was appointed Reader at the University of Kent in 1977, and since 1987 he has been Professor of Radio Communications, now Professor Emeritus.